Table 1 Comparison of bunching relative to first satellite for a group of satellites launched with equal ΔV's vs a group launched with unequal ΔV's

Satellite, n	$V_n - V_{n-1}$, fps	Drift rate, deg/day	Times of bunching after injection, days
2	5	1.35	266.67
3	5	2.70	133.33
4	5	4.05	88.89
5	5	5.40	66.67
6	5	6.75	53.33
7	5	8.10	44.44
2	3	0.81	444.44
3	2	1.35	266.67
4	2	1.89	190.48
5	4	2.97	121.21
6	2	3.51	102.56
7	4	4.59	78.43

$\omega = 0.000291$ rad/sec and $\sin\omega t = \omega t - (\omega t)^3/6$, we get $Z \simeq 3.4$ naut miles at 1.22 hr after injection.

The relative drift rate of one satellite with respect to another satellite moving with period P (in hr) is 8640 $(\Delta P/P^2)°$/day or 1080 $(\Delta V/V_c)°$/period, where ΔP is the difference in period.

The relative drift rate of two consecutive satellites is 1°.35 per day. The last satellite will therefore be drifting at 8°.1 per day from the first one. Thus, after its first revolution, the earliest duration for one satellite to be overtaken by another satellite is 44.44 days, and the first satellite overtakes the last one when they are 280° in their orbit from the injection point. After 266.67 days at an angular distance of 240° from the injection point, each one of the seven satellites is being overtaken by one another. Thus, every 266.67 days all of the satellites bunch together in the same direction and are radially separated by 8 naut miles each. The results are summarized in the first group in Table 1 and in Fig. 1a. Note that the maximum separation of any satellite relative to another cannot exceed 180°, and hence the top horizontal lines in Figs. 1a and 1b represent maximum separation and the bottom horizontal lines represent bunching. The times of mutual bunching between other satellites can easily be read from the figure. As for example, satellites 2, 3, 5, and 6 bunch together among themselves at every 88.89 days as seen from Fig. 1a.

The bunching can be minimized by choosing random differential velocities; for example, let us deploy 7 satellites with $V_n - V_{n-1} = 3$, 5, 7, 11, 13, and 17 fps, respectively. The results are shown by the lower group in Table 1 and in Fig. 1b. Bunching is greatly reduced, and the total increment in velocities is now only 56 fps, as compared to 105 fps for the previous case.

Thus, if random differential velocities are properly chosen, we can reduce bunching to the minimum and at the same time ensure a suitable distribution of the satellites in their orbit to provide the desired coverage for communication links spread throughout the globe.

References

[1] Rinehart, J. D. and Robbins, M. F., "Characteristics of the service provided by the communications satellite in uncontrolled orbits," Bell System Tech. J. **XLI**, 1621–1670 (1962).

[2] Nigam, R. C., "Orbital aspects of deployment of satellites," J. Astronaut. Sci. **XI**, 37–45 (1964).

[3] Jensen, J., Townsend, G. E., Kraft, J. D., and Kork, J. D., *Design Guide to Orbital Flight* (McGraw-Hill Book Co., Inc., New York, 1962), p. 156.

A "Spark-Plug" Starter for Arc Plasma Generators

T. A. Barr Jr.* and R. F. Mayo†
U. S. Army Missile Command, Redstone Arsenal, Ala.

Accurately timed and consistent, simultaneous starting of two or more arc-type plasma generators[1] was required for plasma experiments under a wide range of ambient pressures, some as low as 10^{-4} torr, and open-circuit voltages as low as 200 v d.c. with an arc gap of $\frac{3}{8}$ to $\frac{5}{8}$ in. A high-frequency voltage across the electrodes was satisfactory except that insulation failure resulted. Squibs and shorting links were considered to be unsatisfactory because of the many problems associated with their use. Figure 1a shows an arc starter, which meets the above requirements. A high voltage between the spark-plug tip and the grounded seat causes a transient, high-current arc to form in the channel in the plastic insert. Material vaporized from the channel wall is heated in the arc and ejected as a tongue of plasma into the electrode gap of the plasma generator. The conductivity of the ejected gas is high enough to initiate the arc in the plasma generator. The only modification to the plug is the removal of the ground electrode; any type with a protruding center insulator but without a built-in resistor will do. The plastic insert is made of any one of several plastics (e.g., Lucite, polyethylene, or the fluorocarbon polymers), which do not shatter under the electrical or other stresses developed in the starter. The insert is essential for consistent operation of the starter. The replaceable seat is a washer made of copper, stainless steel, or other noncorroding metal; it is not absolutely necessary but is convenient and prevents wear on the permanent housing.

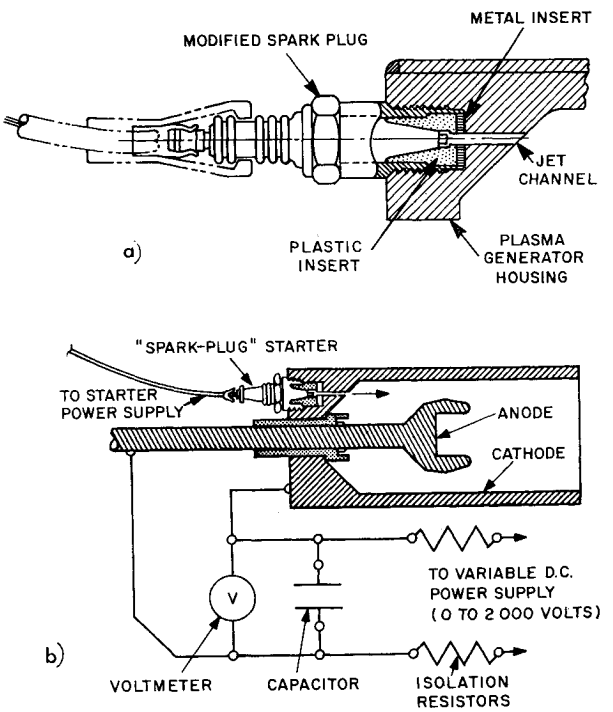

Fig. 1 a) Cross-sectional diagram of an arc starter; b) circuitry for performance characteristics experiment; arc ignition occurs near the point of minimum separation between anode and cathode.

Received February 16, 1965; revision received April 5, 1965.

* Chief, Plasma Physics Branch, Physical Sciences Laboratory, Directorate Research and Development. Member AIAA.

† Research Physicst, Plasma Physics Branch, Physical Sciences Laboratory, Directorate Research and Development.

Starter Control and Power Supply

Figure 2 shows the basic electrical equipment plus two starter modules. Additional modules can be added; the maximum number is limited essentially by the current capacity of the grounding circuit. Two features of the starter system are noteworthy: 1) The starter plugs are at or very near ground potential on both of the contacts except during the actual ignition operation; the IR drop and induced voltage in the coils L create a small transient voltage on the plugs which disappears as soon as the condensers C are charged; and 2) when the switch S_1 is moved to the discharge position, the full voltage of each condenser appears across its associated spark plug. Since this action completes a common ground return for all of the circuits, the ignition of all of the sparks is practically simultaneous. Oscilloscope records have shown that the delay time between the two starters tested is less than 0.1 μsec.

Since the charging rate for the condensers may temporarily overload the capacity of the power supply when S_1 is returned to the charge position, current limiting resistors R_1 and R_2 were placed in the 115-v-a.c. input leads. The switch S_1 is solenoid-operated through an insulating coupling (Lucite rod); S_1 is "homemade" to match the voltage and current requirements of the system. If accurate timing of ignition in the starter is required, a thyratron can be inserted (see dotted lines in Fig. 2), and the plasma generators can be programed to start during the time of travel between opening and closing of S_1. The thyratron, when fired, serves the same purpose as the switch in completing the ground return line.

The induction coils L are the secondary windings of neon-sign transformers rated at 30 kv, 30 ma. The condensers C are nominally rated at 20 kv, 1 μfarad and will stand shorting when fully charged. The switches labeled S_2 are part of the interlock system and are used to short the high-voltage condensers when they are not in use. Coaxial cables (RG 8/U) connect the condensers to the spark plugs (feed-through insulators are at the condenser end rather than coaxial fittings). This system is fitted with remote and local firing options and has safety interlocks in both primary and secondary power circuits to protect personnel from the condensers.

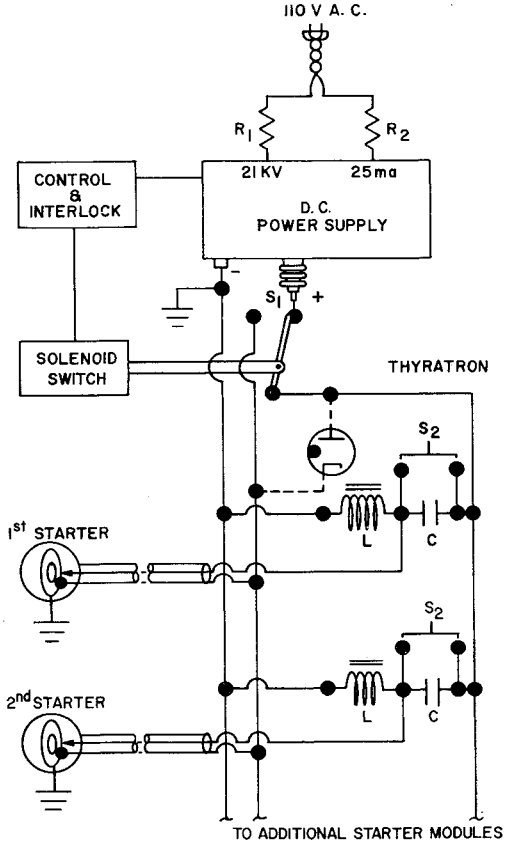

Fig. 2 Circuit diagram for starting system; ignition is performed by solenoid switch Si or by the combination of Si and optional thyration.

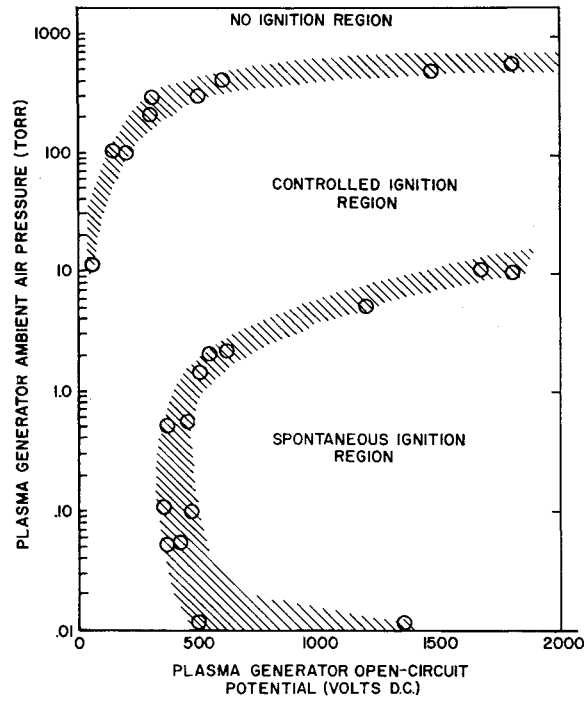

Fig. 3 Zones of spontaneous arc ignition, starter controlled ignition, and no ignition of potential vs ambient pressure map.

Starter Performance

The performance characteristics may be described in terms of the open circuit on the arc plasma generator and the pressure of the gas in the generator before ignition of the arc. The arc rotates on the periphery of the anode (Fig. 1b) under the influence of electromagnets. Rather than have the arc start and run after each ignition, a 2500-v, 4-μfarad condenser is arranged to discharge across the arc gap in place of the power supply. The anode-to-cathode potential difference was measured with an electrostatic voltmeter.

In each test the air pressure in the arc chamber was set, the condenser was charged, and the starter was activated. If the condenser discharged, the generator was considered to have been started. Open-circuit voltage across the generator was initially set at 50 v d.c. (the minimum potential tested) and raised in 50- and 100-v increments until the condenser discharged when the starter was activated. In this manner a crude ignition curve, such as the upper hashed curve in Fig. 3, was obtained. The lower hashed curve is the voltage required to cause spontaneous current leakage between the electrodes of the arc plasma generator. (In this condition it appeared that a very-low-current discharge occurred, since the condenser did not show a tendency to discharge more than a few volts.) The experiments were repeated with an 8-oe magnetic field from the electromagnets. Within the rather low accuracy of this experiment, no difference was noted in ignition points for the plasma generator with or without the field.

To explore the mechanism of ignition, the starter was removed from the plasma generator and fastened to one leg of a 1-in. glass cross, and two pairs of #18 bare copper electrode wires were placed in the line-of-sight of the starter, one 0.2 cm from the outside face of the starter and the other 14.5 cm farther away. The electrodes in each pair were 1 cm apart. Four tests were conducted as shown in Table 1. The electrode

Table 1 Ignition mechanism tests; ambient pressure, 10^{-3} torr

Number of capacitors used on one starter	Electrode potential, v	Ignition delay, μsec	Ignition velocity cm/sec
1	150	2	7.2×10^6
1[a]	150	1.2	1.3×10^7
2	150	1.2	1.2×10^7
2	300	<0.2	$>7.3 \times 10^7$

[a] In this case the 20-kv power supply was left on the condenser for several minutes instead of the usual 10–20 sec. Each condenser was rated at μfarad at 20 kv.

potential shown is the drop across each pair of electrodes which is supplied by a charged condenser. The ignition delay is the time between the discharge of one condenser through the pair of electrodes nearest the starter and the discharge of a second condenser through the other pair. The ignition velocity is the separation distance between a pair of electrodes divided by the ignition delay time. No clear case can be made for either ignition by plasma injection or photoionization, but the ignition in the last of the four tests probably was caused by photoionization, and the first three probably were caused by plasma injection.

Conclusion

The device described in this note has proved to be a reliable and rapid starter for arc plasma generators. Ignition of the arc appears to occur in less than 1 μsec, if the pressure and open-circuit arc voltage are in the domain specified in Fig. 3. Small axial magnetic fields do not significantly change the domain. Within the limits of accuracy of this experiment, no observable difference in arc ignition times was found between one arc and the other in a two-arc system. No starter voltages appear directly across the plasma generator electrodes or insulators to cause short circuit failures. This starter system will be used in a six-arc, 8000-kw plasma facility, which is under construction.

Reference

[1] Mayo, R. F., Wells, W. L., and Wallio, M. A., "A magnetically rotated electric arc air heater employing a strong magnetic field and copper electrodes," NASA TN D-2032 (November 1963).

Lorentz Drag: An Engineering Approximation

ROBERT R. BASS* AND THOMAS P. ANDERSON†
Northwestern University, Evanston, Ill.

Nomenclature

A = flow area
h = enthalpy
H_0 = total enthalpy (constant)
L = length of duct
$\dot{m}$ = mass flow rate
M_e = exit Mach number
M_0 = inlet Mach number
P = fluid pressure
R = body radius
δR = shock standoff distance
γ = ratio of specific heats
ρ = fluid density
σ = electrical conductivity
ξ = volume

Received February 24, 1965; revision received March 26, 1965. This work was supported in part by NASA under Grant No. NSG 547.

* Graduate Student, Department of Mechanical Engineering and Astronautical Sciences, Gas Dynamics Laboratory. Member AIAA.

† Associate Professor and Assistant Director, Gas Dynamics Laboratory. Member AIAA.

Introduction

DURING re-entry there is a need for a large drag to decelerate the vehicle. A proposed method for increasing the drag is known as magnetoaerodynamic drag (MADD). The ionized gas behind the bow shock interacts with a strong magnetic field producing an additional $\mathbf{J} \times \mathbf{B}$ force. It is possible to produce the magnetic field on board the re-entry vehicle without excessive additional weight by using cryomagnets. Figure 1, similar to one in Ref. 1, is a schematic of this problem. The $\mathbf{J} \times \mathbf{B}$ force is henceforth called the Lorentz drag (D_L) or MADD. Ericson and Maciulaitis[2] have investigated this problem in order to determine the possibility of using the field-flow interaction as a means of flight control. They have given a rather extensive treatment of regimes of large interaction where flight control can be accomplished using the lift component of the force produced when the magnet is swiveled. This note outlines a method of estimating the relative magnitude of MADD or "magnetic braking" and is concerned with the drag component of the force rather than the control component. There is a need for some simplifying approach to this problem because of the complications introduced by chemical reactions, ionization recombination, and the magnetic interaction at hypersonic speeds.

Heims[3] has suggested an annular stream-tube technique for another blunt-body problem. His streamtube is approximated by a hyperbolic nozzle. Perhaps this approach could be used for a monatomic gas flow using a treatment similar to Bray and Wilson.[4,5] However, for multicomponent air, this approach would be more difficult and less applicable. The approach used herein is less difficult because of the many simplifying assumptions. The flow is approximated by a constant-area duct flow with constant conductivity. Two regions are considered: a subsonic high-conductivity nose region and a low-conductivity supersonic region, which extends from the sonic line to the body shoulder ($\theta = 90°$) (Fig. 1).

Governing Equations

Using a right-handed Cartesian coordinate system with flow V in the X direction, magnetic induction or field B_Y in the Y

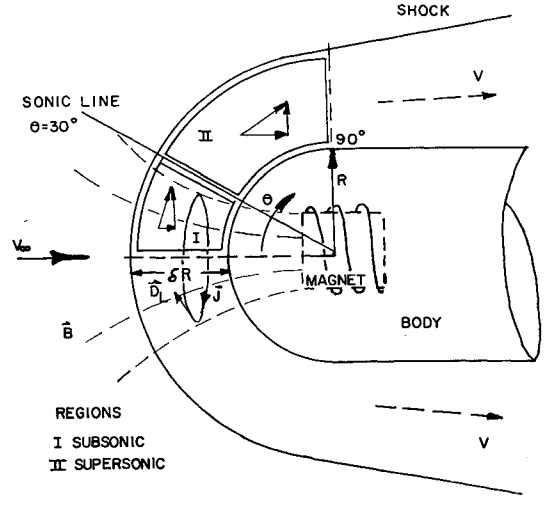

Fig. 1 Flow geometry for MADD analysis showing channel approximation idea in two distinct regions.